

Probing the atmosphere of the bulge G5III star OGLE-2002-BUL-069 by analysis of microlensed H α line *

A. Cassan^{1,2}, J.P. Beaulieu^{1,2}, S. Brillant³, C. Coutures^{1,2,4}, M. Dominik^{1,5}, J. Donatowicz⁶, U.G. Jørgensen^{1,7}, D. Kubas^{1,8}, M.D. Albrow^{1,9}, J.A.R. Caldwell^{1,10}, P. Fouqué^{1,11,12}, J. Greenhill^{1,13}, K. Hill^{1,13}, K. Horne^{1,5}, S. Kane^{1,5}, R. Martin^{1,14}, J. Menzies^{1,15}, K.R. Pollard^{1,9}, K.C. Sahu^{1,10}, C. Vinter⁷, J. Wambsganss^{1,8}, R. Watson^{1,13}, A. Williams^{1,14}, C. Fendt⁸, P. Hauschildt¹⁶, J. Heinmueller⁸, J. B. Marquette², and C. Thurl¹⁷

¹ PLANET collaboration member

² Institut d'Astrophysique de Paris, 98bis Boulevard Arago, 75014 Paris, France

³ European Southern Observatory, Casilla 19001, Vitacura 19, Santiago, Chile

⁴ DSM/DAPNIA, CEA Saclay, 91191 Gif-sur-Yvette cedex, France

⁵ University of St Andrews, School of Physics & Astronomy, North Haugh, St Andrews, KY16 9SS, United Kingdom

⁶ Technical University of Vienna, Dept. of Computing, Wiedner Hauptstrasse 10, Vienna, Austria

⁷ Niels Bohr Institute, Astronomical Observatory, Juliane Maries Vej 30, DK-2100 Copenhagen, Denmark

⁸ Universität Potsdam, Astrophysik, Am Neuen Palais 10, D-14469 Potsdam, Germany

⁹ University of Canterbury, Department of Physics & Astronomy, Private Bag 4800, Christchurch, New Zealand

¹⁰ Space Telescope Science Institute, 3700 San Martin Drive, Baltimore, MD 21218, USA

¹¹ Observatoire de Paris, Section de Meudon, LESIA, 5 pl. Jules Janssen, 92195 Meudon Cedex France

¹² Observatoire Midi-Pyrénées, UMR 5572, 14, avenue Edouard Belin, F-31400 Toulouse, France

¹³ University of Tasmania, Physics Department, GPO 252C, Hobart, Tasmania 7001, Australia

¹⁴ Perth Observatory, Walnut Road, Bickley, Perth 6076, Australia

¹⁵ South African Astronomical Observatory, P.O. Box 9 Observatory 7935, South Africa

¹⁶ Hamburger Sternwarte, Gojenbergsweg 112, 21029 Hamburg, Germany

¹⁷ RSAA, Mount Stromlo and Siding Spring Observatories, ANU, Cotter Road, Weston Creek, Canberra, ACT 2611, Australia

Received ; accepted

Abstract. We discuss high-resolution, time-resolved spectra of the caustic exit of the binary microlensing event OGLE 2002-BUL-69 obtained with UVES on the VLT. The source star is a G5III giant in the Galactic Bulge. During such events, the source star is highly magnified, and a strong differential magnification around the caustic resolves its surface. Using an appropriate model stellar atmosphere generated by the NextGEN code we obtained a model light curve for the caustic exit and compared it with a dense set of photometric observations obtained by the PLANET microlensing follow up network. We further compared predicted variations in the H α equivalent width with those measured from our spectra. While the model and observations agree in the gross features, there are discrepancies suggesting shortcomings in the model, particularly for the H α line core, where we have detected amplified emission from the stellar chromosphere as the source star's trailing limb exited the caustic. This achievement became possible by the provision of the OGLE-III Early Warning System, a network of small telescopes capable of nearly-continuous round-the-clock photometric monitoring, on-line data reduction, daily near-real-time modelling in order to predict caustic crossing parameters, and a fast and efficient response of a 8m-class telescope to a "Target-Of-Opportunity" observation request.

Key words. Techniques: gravitational microlensing – Techniques: high resolution spectra – Techniques: high angular resolution – Stars: atmosphere models – Stars: individual (OGLE 2002-BUL-69)

1. Introduction

Near extended caustics produced by binary (or multiple) lenses, the source star undergoes a large total magnification in bright-

ness. Furthermore, its surface is differentially magnified, due to a strong gradient in magnification. The relative lens-source proper motion is typically slow enough to allow the light curve to be frequently sampled. This translates to a high spatial resolution on the source star's surface and hence permits its radial brightness profile to be inferred from the observations. Over the past four years, coefficients characteriz-

Send offprint requests to: beaulieu@iap.fr

* Based on observations made at ESO, 69.D-0261(A), 269.D-5042(A), 169.C-0510(A)

ing linear or square-root limb-darkening profiles have been obtained with the microlensing technique for several Bulge giants and sub-giants (Albrow et al. 1999b, 2000, 2001b,a; Afonso et al. 2000; Fields et al. 2003). A new generation of stellar atmosphere models (Orosz & Hauschildt 2000) have revealed limb-darkening laws that are significantly different from the traditional analytic ones (Bryce et al. 2003; An et al. 2002; Claret & Hauschildt 2003).

The centre to limb variation of spectral lines can show markedly different behaviour from that of the continuum. Most moderately strong and weak lines weaken towards the limb, but resonant scattering lines can vary in a much more pronounced way. In cool giants, H β , being formed lower in the atmosphere, is more limb-darkened than H α . TiO and CaII show strong variations, and some lines and bands may even be limb-brightened. Intensive spectroscopic monitoring of a caustic exit at high resolution with high S/N should reveal temporal variations in the equivalent widths of promising spectral lines which can be compared with predictions from stellar atmosphere models (Heyrovský et al. 2000).

We present here the first photometric and spectroscopic monitoring campaign that has successfully been performed at high resolution with dense sampling. Previously, Castro et al. (2001) obtained two KECK spectra of EROS 2000-BLG-5, but missed the trailing limb of the caustic where the effects are stronger, while the data in the qualitative analysis of Albrow et al. (2001a) and later reanalysis by Afonso et al. (2001) involved dense coverage but low resolution. Using a determination of the spectral type of the source star, we have computed the limb-darkening profiles in R and I from appropriate NextGEN synthetic spectra of the source star and fitted a fold-caustic model to our photometric data obtained during the caustic exit. This model has been used here to compute the synthetic spectrum for wavelengths around the H α -line.

A more detailed report on the determination of the stellar parameters and the analysis of other spectral lines will be presented elsewhere (Beaulieu et al. 2004), as will the details of a full binary lens model fit to the PLANET observations of the event (Kubas et al. 2004).

2. OGLE 2002-BUL-69 photometry and spectroscopy

The PLANET collaboration, comprising six different telescopes, namely, SAAO 1.0m (South Africa), Danish 1.54m (Chile), ESO 2.2m (Chile), Canopus 1.0m (Australia), Mt. Stromlo 50in (Australia) and Perth 0.6m (Australia), commenced photometric observations of OGLE 2002-BUL-69 alerted by the OGLE-III early Warning System (Udalski et al. 1994) (<http://www.astrowu.edu.pl/~ogle/ogle3/ews/ews.html>) in early June, 2002. From online data reductions on June 25 it was realised that the event involved a binary lens and a bright giant source star. With the source taking ~ 1.4 days to cross the caustic on entry, it appeared to be an excellent candidate for time-resolved spectroscopy of the caustic exit. Using the predictions based on modeling our photometry, and thanks to excellent coordination with the staff at Paranal, very good coverage was obtained during the caustic exit together with post-

caustic reference spectra. These observations were performed using the UVES spectrograph mounted on Kueyen as part of Target-of-Opportunity and Director's Discretionary time. 39 spectra were obtained alternately in the so-called standard settings, 580 and 860, covering the full 4800 – 10600 Å range at a resolution of 30000 with S/N ranging from 50 to 130. From an analysis of the curve-of-growth of 100 FeI and FeII lines as done by Minniti et al. (2002), and independently from the study of the CaII and Mg lines (Jørgensen et al. 1992), a good fit to all the data was obtained with a plane-parallel model atmosphere having $T_{\text{eff}} = 5000$ K, $\log(g) = 2.5$, $v_{\text{turb}} = 1.5$ km s $^{-1}$, and $[\text{Fe}/\text{H}] = -0.6$, corresponding to a G5III bulge giant star at a distance of ~ 6.3 kpc.

3. Stellar intensity profile

Let $I^{\lambda}(\rho) = \bar{I}^{\lambda} \xi^{\lambda}(\rho)$ denote the specific intensity density for a wavelength λ as a function of fractional radius ρ , where \bar{I}^{λ} is the average intensity density of the source and $\xi^{\lambda}(\rho)$ is a dimensionless function describing the intensity profile. With the transmission function $B^{(s)}(\lambda)$ accounting for the convolution of filter, CCD and atmosphere transmissions, the normalized stellar intensity profile for a filter $\xi^{(s)}$ reads

$$\xi^{(s)} = \frac{\int_0^{\infty} \bar{I}^{\lambda} B^{(s)}(\lambda) \xi^{\lambda}(\rho) d\lambda}{\int_0^{\infty} \bar{I}^{\lambda} B^{(s)}(\lambda) d\lambda} \quad (1)$$

We approximate the source as being comprised of N concentric rings of constant intensity I_i^{λ} . Stellar atmosphere models have been computed with the PHOENIX NextGEN code (Hauschildt et al. 1999, Orosz & Hauschildt 2000) using spherical geometry and spherically symmetric radiative transfer for the stellar parameters given in Sect. 2 at a spectral resolution of 0.05 Å yielding 128 coefficients I_i^{λ} for each wavelength. An interpolation of the corresponding profile function $I^{\lambda}(\rho)$ with a cubic spline provides us with $N = 1000$ coefficients which are equally spaced in $\cos \vartheta = \sqrt{1 - \rho^2}$, where ϑ is the emergent angle, so that the width of the rings of constant intensity decreases towards the stellar limb.

4. Modelling the caustic exit

For the s -th lightcurve of a star observed at a specific observatory in a specific filter, the observed magnitude $m^{(s)}(t)$ reads

$$m^{(s)}(t) = m_S^{(s)} - 2.5 \lg \left\{ A^{(s)}(t) + g^{(s)} \right\} \quad (2)$$

where $m_S^{(s)}$ is the intrinsic source magnitude, $g^{(s)} = F_B^{(s)} / F_S^{(s)}$ is the ratio between background flux $F_B^{(s)}$ and intrinsic source flux $F_S^{(s)}$, and $A^{(s)}(t)$ the source magnification at time t .

The photometric data presented in the lower panel of Fig. 1 show a peak with the characteristic shape resulting from a fold-caustic exit. For a source in the vicinity of a fold caustic, the magnification $A^{(s)}(t)$ can be decomposed (e.g. Albrow et al. 1999a) as $A^{(s)}(t) = A_{\text{crit}}^{(s)}(t) + A_{\text{other}}^{(s)}(t)$, where $A_{\text{crit}}^{(s)}(t)$ denotes the magnification of the critical images associated with

the caustic, and $A_{\text{other}}(t)$ denotes the magnification of the remaining images of the source under the action of the binary lens.

Let us consider a uniformly moving source crossing the caustic within $2\Delta t$ and exiting the caustic by its trailing limb at t_f . If one neglects the curvature of the caustic and the variation of its strength over the size of the source, the magnification of the critical images reads

$$A_{\text{crit}}^{(s)}(t) = a_{\text{crit}} G_f \left(-\frac{t - t_f}{\Delta t}; \xi^{(s)} \right), \quad (3)$$

where $G_f(\eta; \xi^{(s)})$ is the characteristic fold-caustic profile function which solely depends on the shape of the profile intensity $\xi^{(s)}$:

$$G_f(\eta; \xi^{(s)}) = \frac{2}{\pi} \int_{\max(1-\eta, -1)}^{\max(1-\eta, 1)} \frac{1}{\sqrt{\rho_{\perp} + \eta - 1}} \times \times \int_0^{\sqrt{1-\rho_{\perp}^2}} \xi^{(s)} \left(\sqrt{\rho_{\perp}^2 + \rho_{\parallel}^2} \right) d\rho_{\parallel} d\rho_{\perp}. \quad (4)$$

For $|\omega(t - t_f)| \ll 1$, the magnification of the non-critical images can be approximated by

$$A_{\text{other}}(t) = a_{\text{other}} e^{\{\omega(t - t_f)\}} \simeq a_{\text{other}} [1 + \omega(t - t_f)] \quad (5)$$

where a_{other} is the magnification at the caustic exit at time t_f and ω measures its variation.

As the region where our generic fold-caustic model is believed to be a fair approximation, we chose the range $2463.45 \leq \text{HJD} - 2450000 \leq 2467$. Restricting our attention to all data sets with more than two points in this region leaves us with 29 points from SAAO and 15 points from UTas in I as well as 98 points from the ESO 2.2m in R , amounting to a total of 142 data points. From a binary lens model of the complete data sets (Kubas et al. 2004) for these observatories and filters, we have determined the source magnitudes $m_S^{(s)}$ and the blend ratios $g^{(s)}$. With the adopted synthetic spectra, we computed the stellar intensity profiles for I and R , and used these for obtaining a fit of the generic fold-caustic model to the data in the caustic-crossing region by means of χ^2 -minimization, which determined the 5 model parameters t_f , Δt , a_{crit} , a_{other} , and ω as shown in Tab. 1. If a classical linear limb darkening is included in the list of parameters to fit (as in Albrow et al. (1999b)), the best fit is obtained with $\Gamma = 0.5$. The modeled light curve and the structure of the residuals of the two fits are given in the three lower panels of Fig. 1. The fit with adopted NextGEN limb darkenings is clearly showing systematic trends at the level of 1-2 %. The same trends in the residuals can be seen from the figure, which suggests some specific features lying in the real stellar atmosphere. We checked whether this discrepancy can be caused by the straight fold caustic approximation, but from running the already mentioned global binary lens model neither the very small curvature of the caustic nor the source trajectory can explain this systematic effect.

Table 1. Model parameters of a fit to data obtained by PLANET with the SAAO 1.0m, UTas, and ESO 2.2m. on the microlensing event OGLE 2002-BUL-69. While source magnitudes $m_S^{(s)}$ and blend ratios $g^{(s)}$ result from a fit involving a binary lens model to the complete data sets, the remaining parameters have been determined from applying a generic fold-caustic model solely to the data taken around the caustic exit ($2463.45 \leq \text{HJD} - 2450000 \leq 2467$).

Parameter	Value	Parameter	Value
$m_S^{\text{SAAO } [I]}$	16.05	t_f (days)	2465.637
$m_S^{\text{UTas } [I]}$	16.05	Δt (days)	0.7297
$m_S^{\text{ESO 2.2m } [R]}$	16.3	a_{crit}	19.60
$g^{\text{SAAO } [I]}$	0.16	a_{other}	7.011
$g^{\text{UTas } [I]}$	0.064	ω (days) $^{-1}$	-0.04519
$g^{\text{ESO 2.2m } [R]}$	0.0083		

5. Comparison between synthetic spectra and spectroscopic data

The fold caustic model derived in Sec. 4 was used to compute the source flux during the caustic exit in order to obtain a synthetic spectrum at each epoch in a consistent way. In Fig. 2 we show the observed and synthetic spectra at two epochs: July 9 at 00h04 and July 9 at 22h59 (trailing limb crossing the caustic).

A first analysis reveals good agreement between UVES and synthetic spectra for the wings part of $\text{H}\alpha$ ($6558 - 6561.8 \text{ \AA}$ and $6563.8 - 6567.6 \text{ \AA}$), whereas a clear discrepancy is observed in its core ($6561.8 - 6563.8 \text{ \AA}$). We note that the chromosphere is not included in the NextGEN calculations. Although it should have a minor influence on the broadband limb darkenings, it will have an effect on the core of the lines like $\text{H}\alpha$. We therefore divided the analysis in two parts: the wings and the core. In order to compare the observed equivalent widths of the $\text{H}\alpha$ -line with the predictions from our synthetic spectrum, we applied an overall scale factor to the equivalent width (1.035 for the wings part and 1.495 for the core part of the line), so that the measurements derived from the fiducial model match the post-caustic observations.

The observed and predicted temporal variations of the equivalent widths of both the wings and the core of $\text{H}\alpha$ are plotted in the upper part of Fig. 1. Note at the beginning a small short-term decrease, when the leading limb hits the caustic, followed by little variation while the source centre crosses. There is however a marked change when the trailing limb exits the caustic. The spectral profile of the core is not well matched by the model spectrum; both the width and the depth disagree. Furthermore, the differential variation in flux between the centre and the limb is not well reproduced, even after the scale factor has been applied. However, a better fit is obtained to the wings. Both parts of the line show larger equivalent width variations than predicted by the model.

Last but not least, in the spectrum corresponding to July 10, 02h58 shown in Fig. 3, for which the exposure started 10 min-

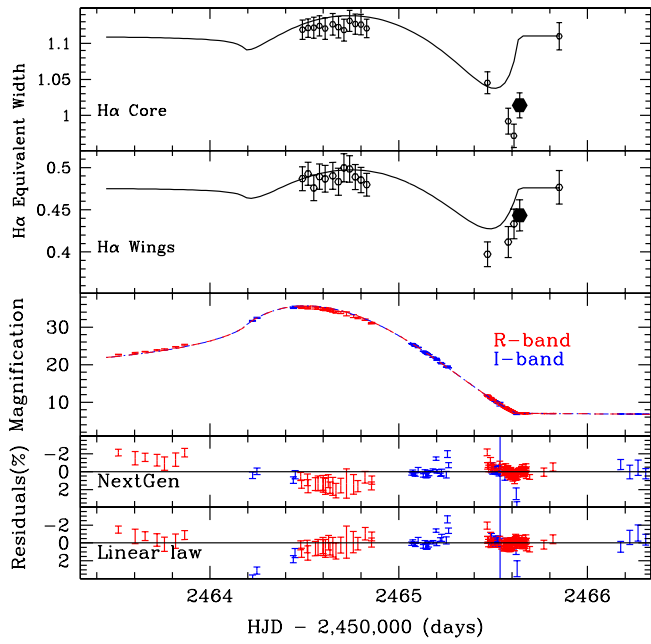


Fig. 1. Equivalent-width variation of the $H\alpha$ core (top panels) and wings (second panel from the top); the open circles in the plots of the equivalent-width variation correspond to our UVES data, while the adjoining solid lines represent the model predictions over the course of the caustic passage. The big dots correspond to the spectra of July 10, 02H58. Third panel: model light curves and photometric data, where R-band data are plotted in red and I-band data in blue; model residuals from the chosen NextGen atmosphere (fourth panel) and from the linear limb-darkening law (bottom panel), with the same color convention. The model parameters can be found in Tab. 1. The majority of model residuals are below the 2 % level.

utes before the source exited the caustic and ended 10 minutes after, we clearly note a strong deviation in the core of the line but a much smaller one in the wing. This is consistent with the signature in $H\alpha$ of material moving outward through the giant source star's chromosphere ($H\alpha$ emission line) with a velocity of $\approx 7 \text{ km s}^{-1}$, and the signature being amplified at the very end of the caustic exit.

Acknowledgements. We are very grateful to OGLE-III for their Early Warning System (EWS), to the observatories that support our science (European Southern Observatory, Canopus, CTIO, Perth, SAAO) via the generous allocations of time that make this work possible. For this particular VLT follow up exercise, we are expressing our highest gratitude to the ESO staff at Paranal whose flexibility and efficiency was absolutely vital to the success of the observations. The operation of Canopus Observatory is in part supported by the financial contribution from David Warren, and the Danish telescope at La Silla is operated by IJAF financed by SNF. JPB acknowledges financial support via award of the "Action Thématique Innovante" INSU/CNRS. MD acknowledges postdoctoral support on the PPARC rolling grant PPA/G/O/2001/00475.

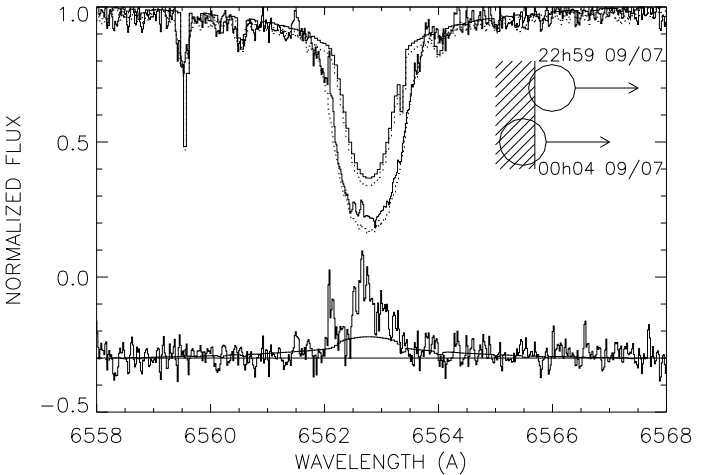


Fig. 2. Upper panel: two UVES spectra (two lower curves) corresponding to July 9, 22h59 ($\text{HJD} - 245000 = 2465.47$, solid line) and July 9 at 00h04 ($\text{HJD} - 245000 = 2464.51$, dotted line), as well as two computed synthetic spectra at the same epochs (the two upper solid and dotted curves). Lower panel: fractional difference $\delta F^\lambda = 2(F_{00h04}^\lambda - F_{22h59}^\lambda)/(F_{00h04}^\lambda + F_{22h59}^\lambda)$ (lower solid line) for wavelengths in the vicinity of the $H\alpha$ line shifted by -0.3. Both the observations and the model are shown. On the upper right, we show the relative position of the source star at each epoch with respect to the fold caustic shown as dashed.

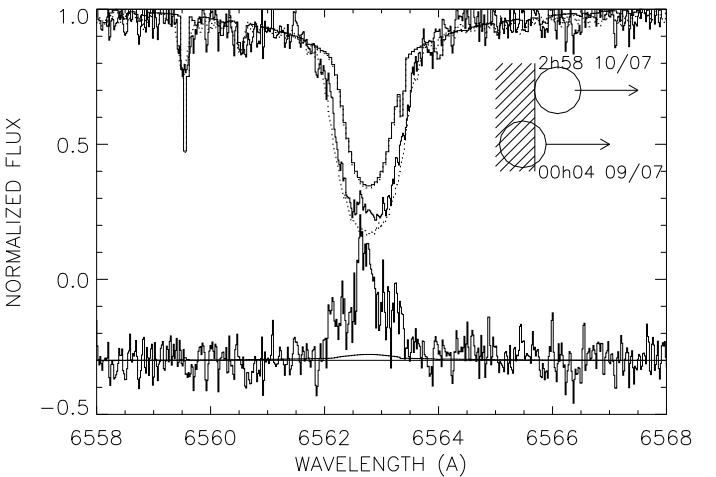


Fig. 3. Same Legend as Fig. 2 but for the pair of spectra July 9 at 00h04. and July 10, 02h58. Notice the strong signature of the chromospheric $H\alpha$ emission.

References

- Afonso, C., Albert, J. N., Andersen, J., et al. 2001, A&A, 378, 1014
- Afonso, C. et al. 2000, ApJ, 532, 340
- Albrow, M. D. et al. 1999a, ApJ, 522, 1022
- . 1999b, ApJ, 522, 1011
- . 2000, ApJ, 534, 894
- . 2001a, ApJ, 550, L173
- . 2001b, ApJ, 549, 759

An, J. H. et al. 2002, *ApJ*, 572, 521
Beaulieu, J. P. et al. 2004, in preparation
Bryce, H. et al. 2003, *A&A*, 401, 339
Castro, S. et al. 2001, *ApJ*, 548, L197
Claret, A. & Hauschildt, P. H. 2003, *A&A*, 412, 241
Fields, D. L., Albrow, M. D., An, J., et al. 2003, *ApJ*, 596, 1305
Heyrovský, D., Sasselov, D., & Loeb, A. 2000, *ApJ*, 543, 406
Jørgensen, U. G. et al. 1992, *A&A*, 261, 263
Kubas, D. et al. 2004, in preparation
Minniti, D., Barbuy, B., Hill, V., et al. 2002, *A&A*, 384, 884
Orosz, J. A. & Hauschildt, P. H. 2000, *A&A*, 364, 265
Udalski, A., Szymanski, M., Kaluzny, J., et al. 1994, *Acta Astronomica*, 44, 227